Available online at www.sciencedirect.com
ScienceDirect
Applied Catalysis B: Environmental 79 (2008) 323–333
APPLIED CATALYSIS B: ENVIRONMENTAL
www.elsevier.com/locate/apcatb

Effect of acid and base sites on the degradation of sulfur mustard over several typical oxides

Hairong Tang, Zhenxing Cheng *, Haiyan Zhu, Guomin Zuo, Ming Zhang

The No. 3 Department, Institute of Chemical Defence, P.O. Box 1048, Beijing 102205, China

Received 19 September 2007; received in revised form 24 October 2007; accepted 31 October 2007
Available online 7 November 2007

Abstract

The reactions of the chemical warfare agent sulfur mustard (HD) degradation over CaO, MgO, SiO_2, Al_2O_3, HZSM-5, A-Clays were studied. More than 10 kinds of products from the degradation of HD over these oxides were detected and identified by GC-FPD, GC–MS, NMR and UV–vis approaches. All the studied oxides can exhibit reactivity towards destroying HD molecules in air at room temperature. The acid and base sites over the oxides were not entirely poisoned by H_2O and CO_2 in air as evidenced by the acid–base property characterization results. The conserved acid and base sites over the oxides might be the reaction center for degradation of HD molecules. Both degradation activity and product distribution were strongly determined by the strength and density of the acid–base sites and the adsorbed water over the oxides.

Keywords: Mustard; Degradation; Oxide; Acid and base sites

1. Introduction

Decontamination of chemical warfare agents (CWAs) is of great importance for military defense as well as countering terrorism. As the ''king'' of the CWAs, the sulfur mustard (HD) is a permanent agent and difficult to be decontaminated. Its detoxification reactions typically include nucleophilic substitution, elimination of HCl and oxidation through cleavage of C–Cl and S–C bond [1]. Therefore, the decontamination efficiency to HD is commonly regarded as a key specification to a decontaminant.

The oxide powder could be used as a universal decontaminant because of its high capacity to adsorb CWAs, and much attention has been focused on improving the reactivity of the oxides towards destruction of CWAs. In the years between 1994 and 1997, Bellamy reported that HD vapor adsorbed on the 13X zeolite and the modified resins could be degraded. Sulfonium ion of $HOCH_2CH_2SCH_2CH_2Cl^-S^+(CH_2CH_2OH)_2$ (CH-TG) over 13X zeolite [2] and DVS (divinyl sulfide) over the resins [3,4] were identified by NMR. In 1997, Bartarm and Wagner [5] stated in a patent that an activated alumina was able to neutralize the droplets of HD, GD (3,3-dimethyl-2-butyl methylphosphonofluoridate or Soman), GB (isopropyl methylphosphonofluoridate or Sarin) and VX (*O*-ethyl *S*-2-(diisopropylamino)ethyl methylphosphonothioate). In 1999, Mawhinney et al. [6] performed an IR study and demonstrated that there was a formation of surface alkoxide species ($CH_3CH_2SCH_2CH_2O$–Al–) when a high area alumina adsorbed 2-chloroethyl sulfide (a simulant as HD) at room temperature in vacuum; Klabunde and co-workers [7–11] reported the reactions of VX, GB, GD and HD over nanosize MgO, CaO and Al_2O_3 with solid-state MAS NMR technique. They found that the product distribution was TG:DVS = 1:1 for HD over AP-MgO [8] and TG:DVS = 1:4 for HD over AP-CaO [9]. In the case of Al_2O_3, the major reaction products of DVS and small amount of TG were also detected [10]. At that time, Wagner and Klabunde thought that the reactivity of nanosized oxides towards the molecules of CWAs was due to higher surface area, greater amounts of highly reactive edge and corner ''defect'' sites, and unusual, stabilized lattice planes in comparison with commercial oxides. In 1999, Wagner and Bartram [12] reported that HD droplets could also be degraded on NaY and AgY zeolites to form both DVS and the cyclic ether 1,4-thioxane.

The reaction mechanism for decontamination of HD, GB, GD and VX dissolved in water or solvent by nucleophilic or base reagents, such as HOO^-, RO^-, HO^-, has been already

* Corresponding author. Tel.: +86 10 69760164; fax: +86 10 69760161.
E-mail address: chengzx04@tom.com (Z. Cheng).

0926-3373/$ – see front matter © 2007 Elsevier B.V. All rights reserved.
doi:10.1016/j.apcatb.2007.10.036

well clarified as reviewed by Yang et al. [1]. It has been convinced that HD will be quickly hydrolyzed into CH and TG and also possibly eliminated into CEVS (2-chlorethyl vinyl sulfide), HEVS (2-hydroyl vinyl sulfide) and DVS in a basic aqueous solution. Therefore, it seems reasonable to expect that both hydrolysis of C–Cl bond and elimination of HCl occur for HD molecule over solid base oxides as in basic solution medium. Fortunately, this idea was successfully achieved by our group with alumina modified by KF, KOH, NaOH and other cationic salts, as stated in 1998 [13]. Nanosize effect could well enhance the reactivity of Al_2O_3 and MgO for degradation of HD molecules [14]. These obtained data were consisted with those published by Wagner et al. [8–10].

In order to elucidate how the acid and base sites affect the degradation of HD molecules, a series of oxides, such as CaO, MgO, SiO_2, Al_2O_3, HZSM-5, A-Clays, were chosen to study the degradation of HD molecules. Acid–base properties of these oxides were characterized, and the degradation products of HD over these oxides were analyzed. The experimental data reported here would contribute to clarify the mechanism for degradation of HD over oxide and should be helpful to develop sorptive decontaminants.

2. Experimental

2.1. Materials

HD has a purity of >99%. The standard derivatives of HD for GC-FPD analysis were commercially purchased (S_2Cl_2) or self-synthesized (TG). All anhydrous solvents were of analytical grade or distilled before use. The gases of He (>99.999%), CO_2 (>99.999%) and NH_3/He (1.26%) were supplied by Beijing Gas Industry. The specifications of the oxides in this paper are shown in Table 1.

2.2. Characterization of the acid and base sites over the oxides

BET surface area and pore volume were obtained by N_2 adsorption (−195 °C) measurements with Autosorb-1C (American Quantachrome Company). After evacuating the sample at 850 °C, isotherms for both physisorption and chemisorption of CO_2 at 50 °C were performed as follows: firstly, to add CO_2 into adsorption system to get isotherm (*C*); secondly, to evacuate to remove physisorbed CO_2; finally, to re-admit CO_2 into the

Table 1
The values of pH, pK_a, pH_{ZPC} and S_{BET} for several typical acid–base oxides

Sample	Remark	pH	pH_{ZPC}	pK_a	Acidity[a] (mmol/g)	Basicity[a] (mmol/g)	S_{BET} (m^2/g)
R-CaO (BJ)	Reagent, amorphous, Beijing chemical plant	12.56	13.30	15.0–17.2		2.00–2.02	11
R-MgO (BJ)	Reagent, amorphous, Beijing chemical plant	10.45	11.45	9.3–15.0		0.03–0.04	23
N-MgO (TX)	Nanosize/Industry, Taixing nanostructured materials plant	10.42	10.70	9.3–15.0		0.04–0.05	105
R-Al_2O_3 (BJ)	Reagent, amorphous, Beijing chemical plant	7.18	8.00	7.6–9.3			47
N-Al_2O_3 (ZS)	Nanosize/Industry Taixing nanostructured materials plant	7.42	7.50	7.6–9.3			201
γ-Al_2O_3 (SD)	Support/Industry, Shandong chemical plant	9.16	8.75	9.3–15.0			131
γ-Al_2O_3 (TJ)	Support/Laboratory, Tianjin Research Institute of Chemical Engineering	6.00	6.45	0.8–3.3			193
NaOH/Al_2O_3	Impregnant/γ-Al_2O_3 (TJ)	11.86	10.9	3.3–4.4			204
NaCl/Al_2O_3	Impregnant/γ-Al_2O_3 (TJ)	5.83	7.15	−5.6 to −3.0			194
SiO_2 (QD)	Reagent, amorphous, Qingdao Haiyang chemical plant	5.90	5.95	3.3–4.4	0.80		392
A-Clays (SX)[b]	Industry, Shanxi Yang county chemical plant	6.29	4.00	−5.6 to −3.0	0.75		159
HZSM-5 (TJ) (Si/Al = 50)	Support/Laboratory, NaiKai University	6.82	4.30	−5.6 to 3.0	0.44		293

[a] Measured by Hammette indicators.
[b] The formula of A-Clay in this study is $Si_8Al_4O_{20}(OH)_4 \cdot nH_2O$.

system to gain isotherm (W). Sequentially, the difference $C - W$ yielded isotherm (S) represented the amount of chemisorbed CO_2 [15].

NH_3 TPD (temperature programmed desorption of NH_3) experiments were performed in a conventional flow apparatus using a linear quartz reactor (6 mm diameter; 300 mm length); whereas, CO_2 TPD (temperature programmed desorption of CO_2) was conducted with Autosorb-1C. About 0.1 g sample was heated up to 850 °C; this was followed by a decrease down to 700 °C in He flowing at 30 mL/min for 3 h, then the sample was saturated with NH_3/He = 1.26 at 100 °C or CO_2 (>99.999%) at 50 °C for about 1 h in a flow of 30 mL/min. The samples were flushed with He flowing at 30 mL/min for 3 h to clean out the physisorbed NH_3 or CO_2, then the temperature was increased to 800–900 °C, at a rate of 15 °C/min. Desorption process was monitored by OmniStar™ (Balzers Company) connected on line with the reactor.

The pK_a of the oxides was determined by Hammett indicators titration as followed by [16–22]. The ZPC (zero point of charge) for the oxides was determined as being cited in the literature [23]. That is to take a 100 mL conical flask equipped with a ground glass stopper, to mix 10 mL $NaNO_3$ (0.005 mol/L) with different amount of NaOH or HNO_3 to give an aqueous solution of 50 mL with different pH value, to put 0.3 g sample into the solution and to keep stirring at 25 ± 1 °C over one day prior to measure its pH. The determination of pH for the oxides in water was effectuated with pH meter, 0.5 g sample was mixed with about 9.5 mL distilled water to give 10 mL solution in beaker under ultrasonic agitation over 20 min.

2.3. Reaction of HD vapor or droplets over the oxides

The degradation of HD adsorbed from vapor on the surface of oxides was accomplished in air at 25 °C. In a self-constructed vacuum sorption apparatus, about 3.0 g oxide predried at 120 °C was partially saturated with HD vapor; in turn, this sample was divided into several portions. Each portion was then stored in a closed 50 mL conical flask. The degradation of HD droplets over the oxides was effectuated in a similar way. That was to properly mix 1.6 g oxides with 80 μL HD droplets within a glass-dish. The obtained mixture was then collected and sealed into a 50 mL conical flask. *Caution*: HD has high toxicity, and should be handled only by trained personnel using applicable safety procedures. One or several days later, residual HD and its degraded products in the samples were quantitatively determined for the purpose to evaluate the reactivity of different oxides towards HD.

2.4. Analysis of the degradation products of HD over the oxides

In order to identify the products from degradation of HD, acetonitrile was used to extract the sample of HD over the oxides. The extractant was analyzed by GC–MS (Agilent 6890/5973) and GC-FPD (Agilent 6890) as well. A fused-silica capillary column DB-1701 (30 m × 0.25 mm × 0.25 μm) was chosen and a split–splitless injector was used in the splitless mode and maintained at 180 °C. The oven temperature programmed was as follows: initial temperature 50 °C (held for 1.00 min), increased at 10 °C/min to 180 °C, and increased at 5 °C/min to 240 °C. The detector temperature was 250 °C. The separated products were identified by comparison of experimental mass spectra with references or comparison of the retention time with that of standard derivatives of HD.

The sample of HD over the oxides could be extracted with anhydrous ethanol and $CDCl_3$, and then analyzed by UV–vis spectrometry (HP8453) and NMR (JNm-ECA-400). The techniques of ^{13}C solid-state MAS NMR (VARIAN ^{UNITY}*INOVA* 300M) and TG–DTA (PerkinElmer) were also employed to characterize the degraded products of HD droplets over HZSM-5.

3. Results

3.1. Characterization of acid and base sites over the oxides

3.1.1. He TPD (temperature programmed desorption of He)

The studied oxides was carried out without any thermal pretreatment in the experiment of He TPD. The obtained spectra are exemplified in Fig. 1 and summarized in Table 2. Desorption of both CO_2 and H_2O was observed. There was a variety of desorption peaks for CO_2 at different temperatures. Desorption of H_2O around 150 °C should associate with physisorption of H_2O on the oxides, and hereafter H_2O would be produced from dehydroxylation at higher temperature.

3.1.2. CO_2 TPD

Chemisorption of CO_2 by the oxides was measured with Autosorb-1C and the obtained data are listed in Table 2. Chemisorption of CO_2 was found to all the studied oxides. A remarkable increase of chemisorbed CO_2 due to nanosize effect could be observed for both MgO and Al_2O_3. An impregnation of NaOH in alumina was able to improve the amount of chemisorbed CO_2, while impregnation of NaCl lowered it down. Moreover, there existed an obvious difference in the amount of chemisorbed CO_2 for the alumina oxides prepared by different laboratories or plants.

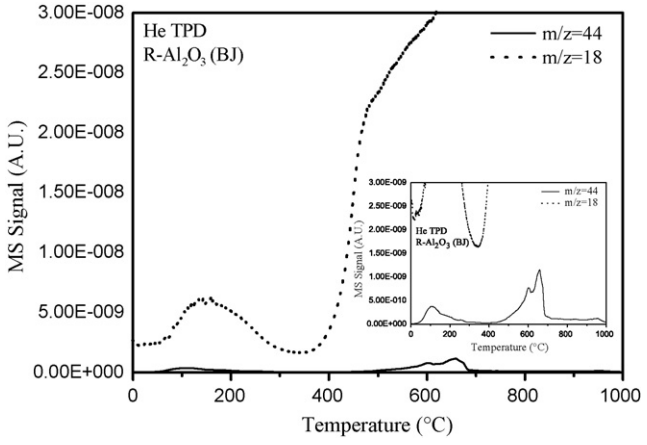

Fig. 1. TPD–MS profiles in a stream of He (30 mL/min, 15 °C/min) for (0.1 g) R-Al_2O_3 (BJ).

Table 2
Temperature for desorption of CO_2 in He TPD and CO_2 TPD and amount of CO_2 chemisorption on the oxides pretreated at 850 and 250 °C

Sample	CO_2 desorption temperature (°C)		CO_2 chemisorption (mmol/g)	
	He TPD	CO_2 TPD	850 °C	250 °C
R-CaO (BJ)	697[a]	665; 114; 183; 239; 284;	0.22	0.08
R-MgO (BJ)	365, 155; 287; 429; 613	641; 118; 181; 237; 281; 316; 704	0.42	0.08
N-MgO (TX)	398; 447; 222; 695	695; 130; 197; 962	2.45	0.01
R-Al_2O_3 (BJ)	659; 102; 602; 954	588; 117; 182; 237; 281; 315; 683; 897	0.08	0.02
N-Al_2O_3 (ZS)	98; 622	688; 127; 195; 248; 939	5.71	0.82
γ-Al_2O_3 (SD)	137; 611	122; 188; 249; 295; 336;	0.05	0.08
γ-Al_2O_3 (TJ)	126	634; 115; 182; 238; 283; 319; 699; 892	0.26	
NaOH/Al_2O_3	154; 658	626; 121; 181; 237; 282; 293; 320	0.48	
NaCl/Al_2O_3	566; 160	607; 119; 181; 242; 284; 320	0.17	
SiO_2 (QD)	602	676; 127; 200; 262	0.12	0.13
A-Clays (SX)	588; 318; 791	207; 267	0.01	0.01
HZSM-5 (TJ)	364; 404; 116; 175; 243	640; 184; 241; 284; 310	0.41	0.04

[a] The underlined numbers were assigned to the temperature of the main desorption peak.

After the oxides had chemisorbed CO_2 at 50 °C, CO_2 TPD was performed and the obtained results are illustrated in Fig. 2 and summarized in Table 2. It was found that there were more peaks in these CO_2 TPD spectra than those directly for He TPD. It is thus likely that chemisorption of CO_2 over the oxides adsorbed H_2O in air should differ from that on the clean oxides surface in vaccum. And that, the pretreatment of the oxides at 850 °C would not only certainly re-activate the base sites poisoned by air, but also probably create some new base sites through dehydroxylation. This could be furthermore supported by an increase of chemisorbed CO_2 when the pretreatment temperature was augmented from 250 to 850 °C. On the other hand, an increase of chemisorbed CO_2 due to nanosize effect, especially which desorbed around 700 °C, was observed for both MgO and Al_2O_3. Both number and temperature of peaks in CO_2 TPD spectra varied with the dissimilarities of alumina oxides. These data were in accordance with the amount of chemisorbed CO_2 determined at 50 °C.

3.1.3. NH_3 TPD

The spectra of NH_3 TPD for the studied oxides are shown in Fig. 3. For CaO and MgO oxides, peaks of TPD originating from NH_3 chemisorbed had not been observed even when adsorption of NH_3 was carried out at room temperature and without pretreating. This would indicate that no acid sites were able to chemisorb NH_3 over CaO and MgO. A trace amount of chemisorbed NH_3 was found in silica oxides. Alumina, A-Clays and HZSM-5, being said acid, gave rise to a similar spectrum, that comprised a NH_3 TPD peak around 200–250 °C, except that there was another shoulder peak at 400 °C for HZSM-5. These experimental results were nearly consisted with the data published in literatures [24–26]. A-Clays and HZSM-5 possessed acid sites of larger number and higher strength than alumina oxides. Different alumina did not give a great difference in either strength or number of acid sites, as that of base sites.

3.1.4. pH, pK_a and pH_{ZPC}

The parameters of pH, pH_{ZPC} and pK_a were determined by immersion of the oxides into distilled water or anhydrous benzene without any pretreatment. These experimental data are listed in Table 1. Base oxides MgO and CaO represented base properties of high strength. Nanosize effect on MgO did not produce a remarkable variation in pH, pH_{ZPC} and pK_a. Acid sites of high strength were found in A-Clays and HZSM-5. The modified alumina could behave different acid–base properties depending on the pretreating method. Silica apparently behaved weakly acid though owning a small number of base sites. It should be noted that the measured pK_a value was different from that reported in refs. [16–19] because of the different pretreating method.

3.2. Degradation of HD over the oxides

All the studied oxides were able to adsorb HD vapor and gave an adsorption isotherm of type II. The saturated sorption quantity (Table 3) was much depended upon their porous structure and surface areas (S_{BET}). More or less amount of irreversible sorption HD was observed for the oxides of high surface when degassing the sample in vacuum ($<10^{-2}$ Pa) at room temperature and extracting HD with solvent as well. When the oxides adsorbed HD vapor of certain amount and had been stored in 30–50 RH% air for 2 days, the oxides of high surface area were proved to evidently degrade adsorbed HD because of a lowering extraction of HD along with time-on-reaction and also the detected products from HD degradation, as presented in Table 3. Silica and A-Clays had a lower reactivity towards degradation of HD. It is worthwhile noting that once a predried HZSM-5 contacted with HD vapor it will turn into yellow from white, and nearly neither HD nor its products could be detected when extracting the sample several hours later.

For the degradation of HD droplets, the studied oxides without exception behaved certain reactivity as being listed in Table 4. Anhydrous $AlCl_3$, $FeCl_3$ and $CuCl_2$, as typical Lewis acids, were also found to quickly degrade HD droplets. Silica, as a neutral oxide, was able to get a higher degradation rate only in H_2O saturated air. Nanosize alumina gave the best degradation rate. It could be significantly improved when adding water into the reaction system (Table 5). An activation

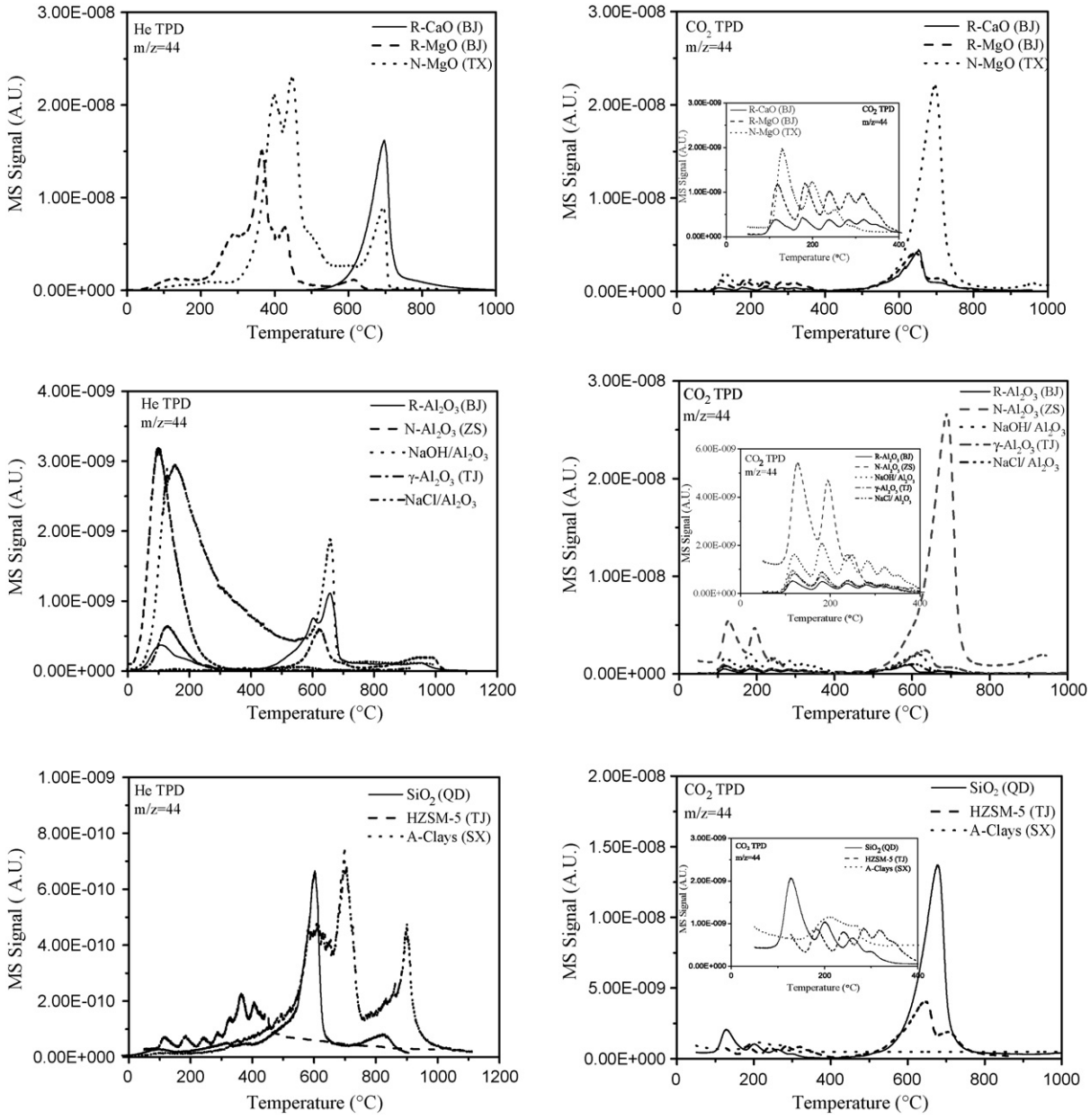

Fig. 2. TPD–MS profiles (left) in a stream of He (30 mL/min, 15 °C/min) for (0.1 g) several typical oxides without any pretreatment and TPD–MS profiles (right) for the samples pretreated at 850 °C and followed by sorption of CO_2 in a flow of 30 mL/min CO_2 at 50 °C.

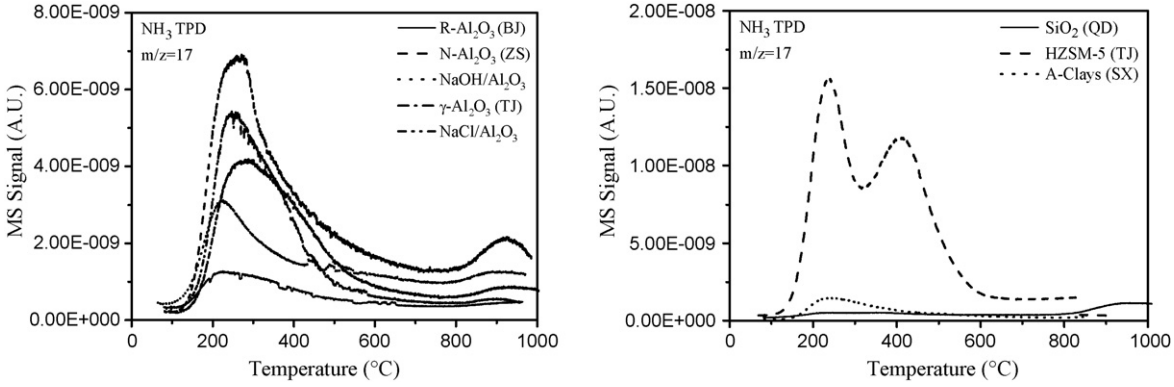

Fig. 3. TPD–MS profiles in a stream of He (30 mL/min, 15 °C/min) for (0.1 g) several typical oxides pretreated at 850 °C and followed by sorption of NH_3 at 100 °C in a flow of 30 mL/min NH_3 (1.26%).

Table 3
Degradation of HD vapor adsorbed on several typical oxides at 25 °C in air of 30–50% RH for 2 days

Sample	a_s[a] (mg/g)	a[b] (mg/g)	Degradation (%)	k (10^{-6} s^{-1})
N-MgO (TX)	90.0	90.0	96.7	8.3
N-Al_2O_3 (ZS)	115.0	105.0	94.5	13.3
γ-Al_2O_3 (TJ)	103.0	90.0	59.0	10.6
NaOH/Al_2O_3		90.0	96.0	36.7
SiO_2 (QD)	898.0	58.8	<10	<0.3
A-Clays (SX)	57.0	57.0	35.1	4.7
HZSM-5 (TJ)	150	90.0	>99.9	>277

[a] Saturated adsorption capacity.
[b] Adsorbed amount for degradation.

energy ΔE_a was estimated to be 34.2 kJ/mol for HD degradation over Al_2O_3 (ZS) in temperature ranges between 10 and 50 °C, and smaller than 85.7 kJ/mol calculated from the hydrolysis data of HD dissolved in water [27].

3.3. Analysis of HD degradation products

3.3.1. GC-FPD and GC–MS analysis

GC-FPD was used to obtain the distribution of products from HD degradation. Nearly 10 kinds of products were detected, and identified by GC–MS as well as reference compounds. The identities of the products are presented in Table 6. The results concerning the distribution of products from degradation of HD are summarized in Table 7. There was no much difference in the distribution of products for the degradation of HD vapor and droplets over the oxides.

For the reaction of HD droplets with Al_2O_3, the products of CH, TG, CEVS, HEVS, 1,4-dithiane, 1,4-oxathiane and sesquimustard are detected and exemplified in Fig. 4. Only CH and TG were initially detected over HZSM-5 and A-Clays, and followed an increase of 1,4-dithiane and sesquimustard. Over $AlCl_3$, S_2Cl_2 was detected in a large amount together with minor CEVS and 1,4-dithiane and decreased along with time-on-reaction, as demonstrated in Fig. 4. The major products detected over MgO were CEVS and HEVS together with small amount of 1,4-dithiane, dially sulfide and O-mustard. But, O-mustard was the major product detected over R-CaO, together with a little 1,4-oxathiane and 1,4-dithiane after stewing for 210 days. CH and TG together with small amount of 1,4-dithiane and sesquimustard were detected over SiO_2. It is worth noting that the amount of sulfur in all the compounds detected only accounted for a ratio less than 60% of HD over the oxides 40 days later.

Table 5
Influence of water on HD droplets (80 μL) degradation over N-Al_2O_3 (ZS) (0.8 g) at 20 °C

H_2O added (mL)	Reaction time (h)	Residue HD (mg)	Degradation (%)	k (10^{-6} s^{-1})
0	240	7.9	92.1	3.1
1.5	17	58.9	42.4	8.9
3.0	17	36.4	64.0	16.7
6.0	17	7.7	92.3	41.7

3.3.2. UV–vis analysis

UV–vis spectra obtained for HD and its degradation products are shown in Fig. 5. For 2 mg/mL HD/C_2H_5OH, two main absorption peaks at 212 and 232 nm with a diminutive peak at 306 nm were found. The concentration of any product from degradation of HD over the oxides was certainly much less than 2 mg/mL due to a possible formation of surface bonded species. Over Al_2O_3 and MgO, the intensity of peaks in the 220 and 300 nm ranges was greatly enhanced and could be associated with C=C bond in CEVS and HEVS. There were two distinct absorption peaks at 310 and 360 nm in the spectrum for HD reaction with SiO_2, which can be possibly assigned to CH and TG. Degradation of HD over HZSM-5, A-Clays and $AlCl_3$ wholly gave a similar UV–vis spectrum with several intense absorption peaks between 250 and 400 nm, which were quite different with that over SiO_2.

3.3.3. ^{13}C MAS NMR and TG–DTA

HZSM-5 would turn immediately from white to yellow once it contacted with HD droplets. At the beginning of HD reacting with HZSM-5, the extraction ratio detected by GC-FPD could reach more than 95%. But 40 days later, the detection ratio of all the sulfur in compounds detected by GC-FPD would sharply lowered down to 21%. Then, it continuously but very slowly decreased within 2 months. The obtained ^{13}C MAS NMR spectrum for the reaction of 80 μL HD droplets with 1.6 g HZSM-5 over 21 days is presented in Fig. 6, and 6 broadened peaks at 43.31, 35.5, 27.1, 57.9, 62.5, 71.3 ppm were observed and no evident variation of spectrum could be produced even 50 days later and upon addition of H_2O in the sample as well. They could possibly be attributed to the compounds with the structures like CH and TG, similar to CH-TG sulfonium ion

Table 4
Degradation of HD droplets over several oxides (80 μL HD mixing with 1.6 g oxide) at 25 °C in air of 30–50% RH for 40 days

Sample	Degradation ratio (%)	k (10^{-6} s^{-1})	Sample	Degradation ratio (%)	k (10^{-6} s^{-1})
R-CaO (BJ)	68.8	0.3	NaOH/Al_2O_3	99.1	15.6
R-MgO (BJ)	65.0	0.3	NaCl/Al_2O_3	94.4	7.2
N-MgO (TX)	88.4	0.6	SiO_2 (QD)	65.3	0.3
R-Al_2O_3 (BJ)	60.2	0.3	SiO_2 (QD)[a]	95.0	6.4
N-Al_2O_3 (ZS)	99.9	16.1	A-Clays (SX)	72.8	3.3
γ-Al_2O_3 (SD)	98.1	12.2	HZSM-5 (TJ)	92.6	5.3
γ-Al_2O_3 (TJ)	99.0	7.8	$AlCl_3$	99.9	9.7

[a] 100% RH for 40 days.

Table 6
Identities of the compounds detected in the experiments

Abbreviation	Name	Structure formulas
S_2Cl_2	Sulfur chloride	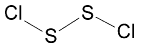
1,4-Oxathiane	1,4-Oxathiane	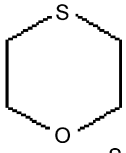
CEVS	2-Chloroethyl vinyl sulfide	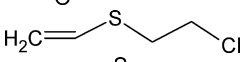
HEVS	2-Hydroxyethyl vinyl sulfide	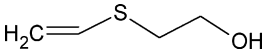
1,4-Dithiane	1,4-Dithiane	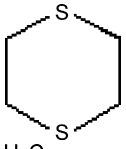
Dially sulphide	2-Propenyl disulphide	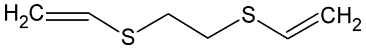
HD	Bis(2-chloroethyl) sulfide	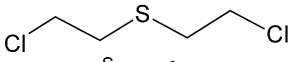
CH	2-Chloro-2′-hydroxydiethyl sulfide	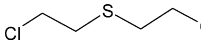
TG	Bis(2-hydroxyethyl) sulfide	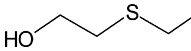
Sesquimustard	1,2-Bis(2-chloroethylthio) ethane	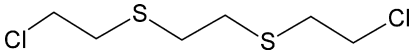
O-Mustard	Bis-[(2-chloroethylthio) ethy] ether	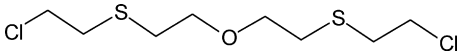

salts as HD droplets reacting with NaY zeolite [12]. TG–DTA profile obtained in N_2 for this sample is presented in Fig. 7. Both loss of weight and endothermal peak around 150 °C should correspond to a desorption of H_2O physisorbed in HZSM-5, while the main peaks between 250 and 450 °C in DTG together with two endothermal peaks at 280 and 310 °C, should associate with the desorption of HD and it's degradation products over HZSM-5. This clearly indicated a strong interaction between the products and HZSM-5 surface.

4. Discussion

4.1. Acid and base properties of the typical oxides

CO_2 TPD and NH_3 TPD are right tools to characterize the strength of base sites and acid sites over the oxides, but trying to attribute each peak to one type of base sites or acid sites would often meet difficulty. Nevertheless, the data obtained could come to a conclusion that there wholly exist base sites on the surface of studied oxides whatever the oxide is acidic, basic and neutral as usually being said. It was observed that CaO and MgO possessed a large number of strong base sites but no acid sites, as evidenced by the chemisorption data of CO_2 and NH_3. The typical amphoteric oxide Al_2O_3 had both acid and base sites. However, the acid oxides like HZSM-5 and A-Clays had strong acid sites of high number, but could have base sites of minor number. The variation of acid and base sites both in number and strength should relate to the distinctness in the aspects of element, solid structure, impurity, particle (nano-) size and others for the oxides studied.

NH_3/CO_2 TPD has well proved the existence of acid–base sites over the oxides. In fact, the acid and base sites over the oxides would partly be poisoned by CO_2 and H_2O in air, as proved by the results of direct TPD in He. Despite of that, the values of pH, pH_{ZPC} and pK_a listed in Table 1 could indicate that the studied oxides still conserved some acid and base sites in air. These data would suggest that both acid and base sites over the oxides were not entirely poisoned by H_2O and CO_2 in air and part of them might be unoccupied.

4.2. Reactions for HD over several typical oxides

An activated alumina [5], nanosize Al_2O_3 [10], MgO [8] and CaO [9] oxides, zeolites like 13X [4], NaY [12] and AgY [12] and F^-/Resins [2,3] have been reported to be reactive towards HD at room temperature in air. However, the above experimental results demonstrated that any oxide seemed possess certain reactivity to degrade HD if one let HD react with the oxide for enough long time (Table 7). Except of low surface reagent oxides, the amount of HD droplets degraded over the oxides (HD/oxide = 1/16) is normally equivalent to or less than the saturated amount of HD adsorbed by the oxides. The degradation rate constant k in first order is in the ranges between 10^{-5} and 10^{-7} s^{-1}. It can be seen from Table 4 that both acid and base sites over the oxides were able to enhance the degradation rate. Al_2O_3 with base sites of larger number and higher strength seemed to have a higher degradation rate.

Table 7
The distribution (%) of products detected by GC-FPD for the reactions of HD over several typical oxides

HD	Reaction time (days)	Oxides	t_R										Degradation (%)	Detection[a] (%)
			2.271 S_2Cl_2	8.616 1,4-Oxathiane	9.026 CEVS	10.422 HEVS	11.988 1,4-Dithiane	13.242 Dially disulphide	14.225 HD	15.183 CH	15.996 TG	18.174 Sesquimustard	24.525 O-Mustard		
Vapor	14	N-Al_2O_3 (ZS)		18.1	29.2	22.2	4.0		11.2	4.8	10.6			90.7	83.1
	40	SiO_2 (QD)					0.1		24.7	31.9	42.3			75.9	97.6
Droplet	210	R-CaO (BJ)		8.3			15.5						76.2	>99.9	0.6
	210	R-MgO (BJ)			3.6	64.2	0.8	20.2				10.2	1.0	>99.9	5.2
	40	N-MgO (TX)		4.3	4.0	57.0	3.3		22.5					88.4	51.5
	210	R-Al_2O_3 (BJ)					1.3	0.5	40.2	24.4	8.8	19.9		98.2	6.5
	14	N-Al_2O_3 (ZS)			11.7	33.7	0.1	13	3.7	14.2	31.7			97.1	56.8
	210	Al_2O_3 (SD)				0.4	1.4		0.1	2.9	77.9			>99.9	7.2
	210	γ-Al_2O_3 (TJ)				0.4	0.2	19.7		0.7	75.8	1.3		>99.9	9.2
	210	SiO_2 (QD)					0.9		43.0	35.0	20.6	0.5		94.4	13.0
	40	A-Clays (SX)		10.2			31.4		22.8	19.5		16.0		98.7	17.5
	40	HZSM-5 (TJ)					15.2		38.4	35.6	7.1	3.6		92.6	21.3
	40	Anhydrous $AlCl_3$	23.4		9.7		26.2		35.3			5.4		78.9	59.8

[a] The ratio of all the sulfur in compounds detected by GC-FPD.

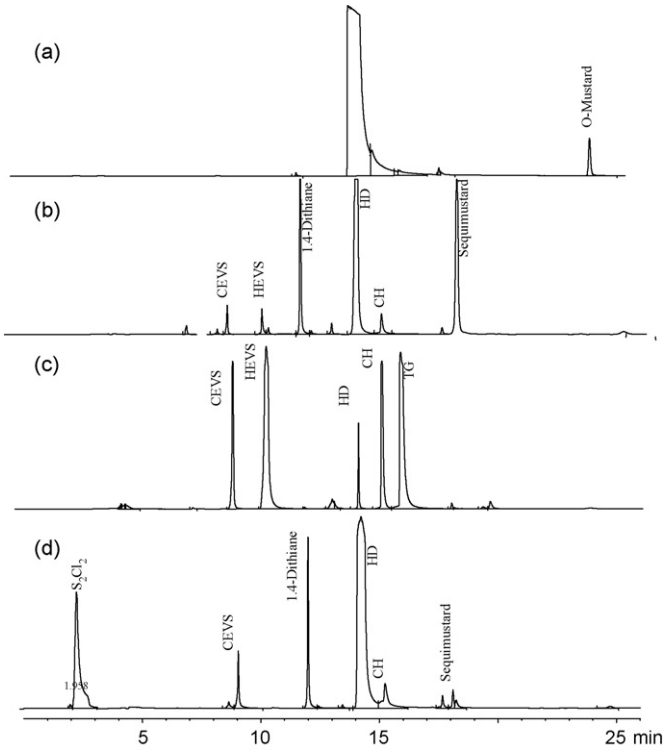

Fig. 4. GC-FPD chromatograms for the residue of HD droplets over (a) R-Al_2O_3 (BJ): 0 days; (b) R-Al_2O_3 (BJ): 40 days; (c) N-Al_2O_3 (ZS): 14 days and (d) $AlCl_3$: 40 days.

The oxide surface in humid air was often partially covered by both H_2O and CO_2 as evidenced by He TPD. Hydrolysis products were detected over all the studied oxides whatever their acid–base properties. It was found that increasing humidity in air or directly adding H_2O into the oxides would accelerate degradation of HD over the oxides. Wagner et al. also found a positive water effect on degradation of HD over nanosize Al_2O_3. In fact, HD can be quickly hydrolyzed into CH and TG once it was dissolved in water and CH-TG sulfonium ion salts and 1,4-dithiane would also possibly be produced when HD relative to H_2O was quite larger and concentrated.

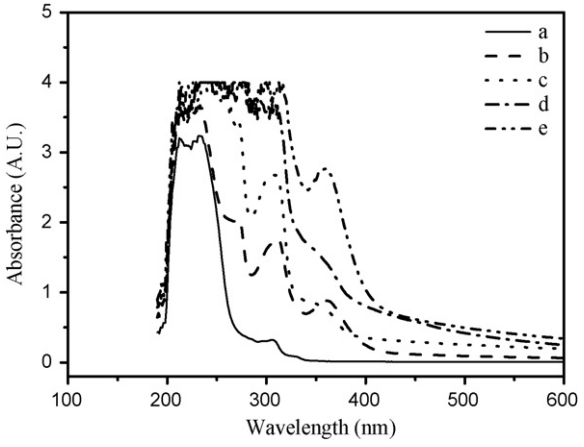

Fig. 5. UV–vis absorption spectra obtained from the residue of (a) HD droplets with (b) SiO_2 (QD), (c) N-MgO (TX), (d) N-Al_2O_3 (ZS) and (e) HZSM-5 (TJ) for 50 days.

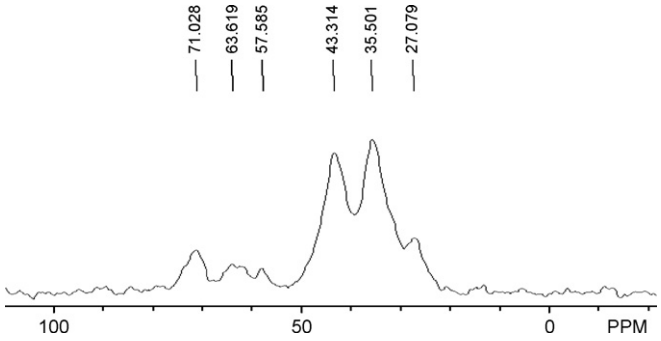

Fig. 6. ^{13}C MAS NMR spectra obtained from the residue of HD droplets over HZSM-5 for 21 days.

The detected products from HD over SiO_2 were mainly consisted of CH and TG. Hence, it seems likely that hydrolysis of HD can proceed so long as H_2O presents over the oxides. The oxide surface certainly provided a large H_2O–HD interface area for HD hydrolysis. It is therefore likely that reactivity of the oxides towards HD was not only depended upon surface acid–base properties but also upon the adsorbed H_2O. On the other hand, both reaction rate constant and activation energy for degradation of HD over the oxides were much smaller than those for hydrolysis of HD in H_2O (1.7×10^{-3} s^{-1}; 85.7 kJ/mol). In general, the diffusion-limited activation energy was lower than 21 kJ/mol [28]. An activation energy ΔE_a was estimated to be 34.2 kJ/mol for the reaction of HD droplets degradation over Al_2O_3 (ZS), which was a little more than that of the general diffusion-limited activation energy due to owning larger molecular weight for HD; However, the reaction was probably still limited by gas-phase diffusion. What we observed fully agree with the findings that HD reactions over nanosize MgO was a fast initial reaction consistent with liquid spreading through the porous nanoparticle aggregates followed by gradual slowing to a steady-state of gas-phase reaction, mediated by evaporation, once the liquid achieves its volume in the smallest available pores reported by Wagner et al. [8].

MAS NMR was mainly used to analyze the products of HD droplets reaction over nanosize Al_2O_3, MgO and CaO by Wagner et al. [7–12], and the products such as TG, H bonded TG, TG-alkoxide, CH-TG, H-2TG, CEVS and DVS seemed to be detected. These degraded products were further confirmed by this work with solvent extraction followed through analysis using GC, GC–MS, UV and NMR analysis methods, but some other products such as HEVS, dially sulphide, 1,4-dithiane, 1,4-oxathiane and sesquimustard were easily identified either. The distribution of these products was strongly depended upon surface acid–base properties. It seemed likely that formation of both (SN) hydrolysis and (E) elimination products profited from base sites while formation of (A/E) addition–elimination products from acid sites, and only (SN) hydrolysis products from neutral surface. On the other hand, the products being extracted and detected by GC-FPD only accounted for a ratio less than 60% of HD reacted over the oxides, and the extraction ratio decreased along with time-on-reaction (Table 7). It would suggest that there probably occurred a formation of stable surface-bonded products, as evidenced by both MAS NMR and DTG–DTA for degradation of HD over HZSM-5 in this work, and suggested by Wagner et al. [10] and Yates et al. [6].

More or less 1,4-dithiane could be detected from HD over the oxides, and even there were sometimes sesquimustard and dially sulphide. It was found that the stronger acidity of the oxide, the higher amount of the above products was produced. It is more surprising that not only two 1,4-dithiane and sesquimustard products but also S_2Cl_2 were detected from HD reaction with $AlCl_3$. This should imply that a cleavage of C–S bond happened in HD molecule. It is known that 1,4-

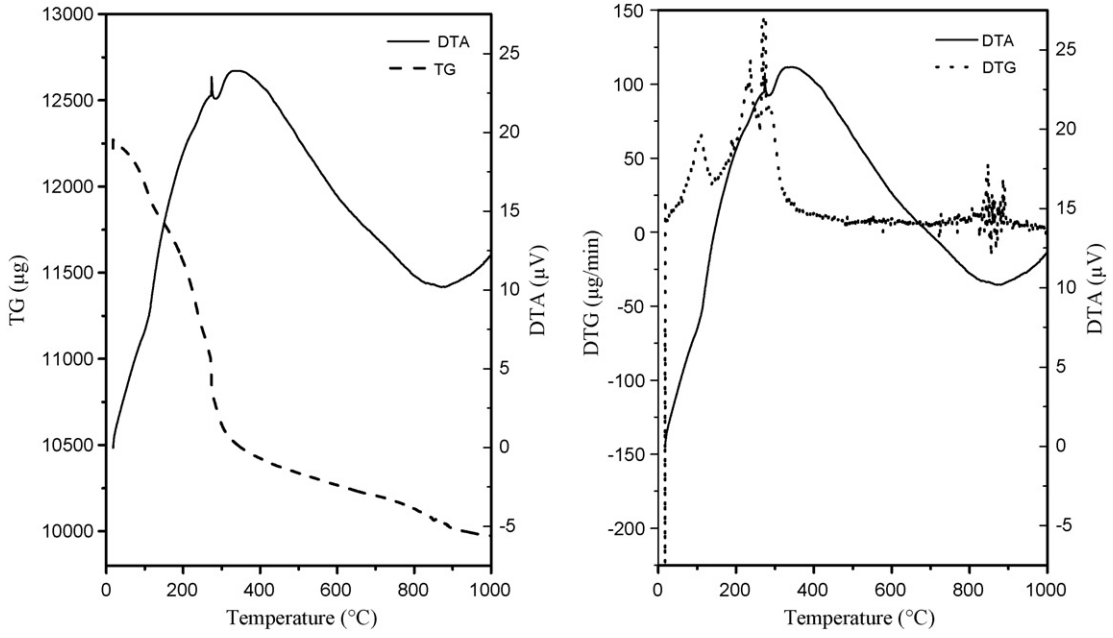

Fig. 7. TG–DTG–DTA profiles for the sample of HD droplets over HZSM-5 for 21 days.

dithiane will be formed in acidic medium for HD hydrolysis. One could thus speculate that either H^+ proton or surface acid site is able to activate C–S bond, evokes addition of one HD molecule to another followed by an inter-molecular elimination of one $ClCH_2CH_2Cl$, two $ClCH_2CH_2Cl$, and finally gives sesquimustard, 1,4-dithiane. If one HD is added to one TG, CH-TG sulfonium ion salt will be produced.

The reaction of HD droplets with nanosize oxides of MgO, CaO and Al_2O_3 could give a product of CEVS, DVS over the base sites on these oxides. The similar products were also detected by Wagner et al. using MAS NMR [8–10]. The detected species was also fundamentally consistent with those observed by Klabunde and co-workers during degradation of 2-CEES over TiO_2, three different types of MgO and $Mg(OH)_2$ [29,30]. DVS and 1,4-oxathiane were detected using MAS NMR for HD reaction with AgY zeolite and the formation of 1,4-oxathiane was presumably attributed to a presence of Ag^+ ion on surface [12]. Some of elimination products, as CEVS, HEVS and dially sulphide, were detected over MgO, Al_2O_3 and $AlCl_3$. HD over $AlCl_3$, possibly undergoes another different reaction pathway to give CEVS, i.e. the C–S bond in HD was activated by $AlCl_3$ Lewis acid, two $CH_2{=}CH_2$ were eliminated from HD molecule to form SCl_2, it followed by decomposition of SCl_2 into S, Cl_2 and S_2Cl_2, one HCl was then possibly eliminated from HD molecule or sulfonium ion through activating C_α–H by Cl_2 to give CEVS. The formation of S product could be supported by the fact that HZSM-5 quickly turned from white into yellow once it sorbed HD of vapor or droplet.

In the case of CaO, the main products detected for HD degradation was O-Mustard and 1,4-dithiane, which were different from those detected over MgO but quite similar to the acid promoted degradation products. This may be imputed to the follows: the elimination of HCl for HD degradation should occur over R-CaO at the beginning of the process, but the S_{BET} of R-CaO was so smaller (11 m^2/g) as that the base sites over R-CaO might quickly be poisoned by the produced HCl during elimination reaction of HD. And then, the surface of oxide will turn from basic into acid along with an accumulation of HCl. The mainly detected products of O-Mustard and 1,4-dithiane can be attributed to the effects of the acid ambient over the poisoned surface of CaO. This was quite similar with the phenomena that O-Mustard would produce when HD store for a certain time.

It is possible that there were different reaction pathways to form the detected products for degradation of HD over the oxides, as shown in Scheme 1. The products containing –OH and C=C groups were probably formed from hydrolysis of C–Cl (SN) and elimination (E) of HCl (C_α–H, C_β–Cl) in HD molecule. Hydrolysis followed by an intra-molecular elimination of HCl would give 1,4-oxathiane, while an inter-molecular elimination of H_2O would form O-mustard. Cleavage of both

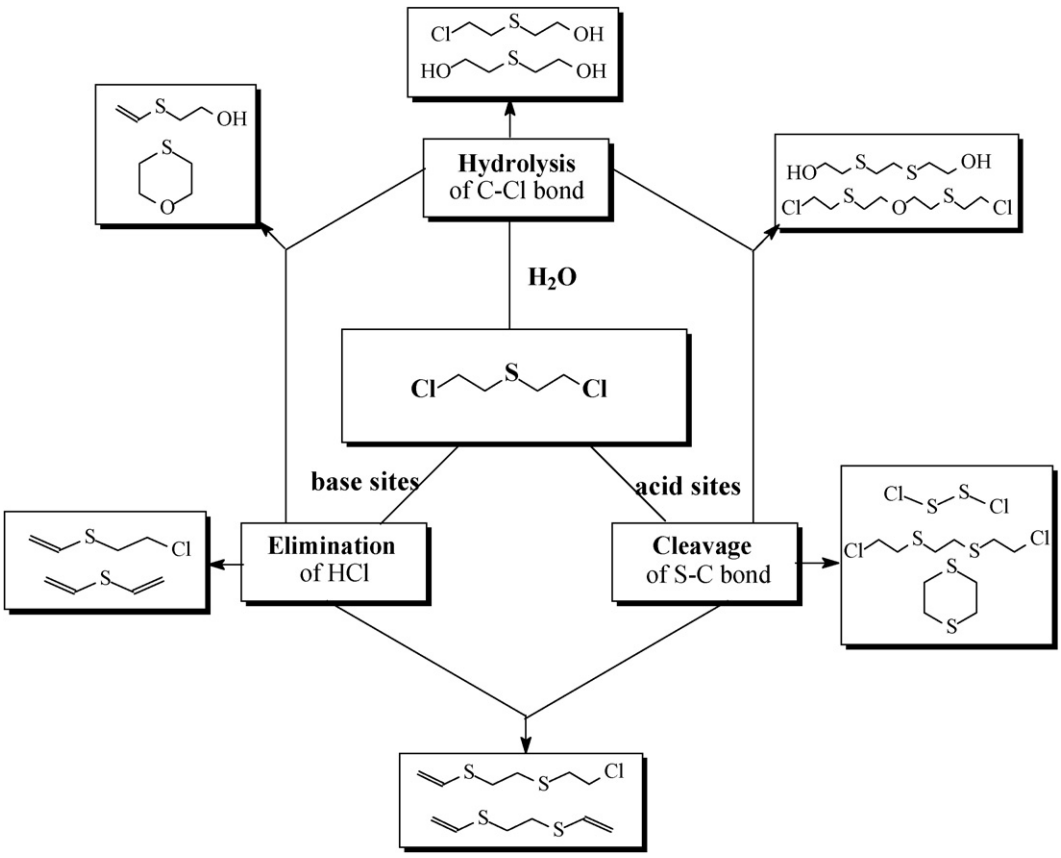

Scheme 1. The role of acid–base sites on the degradation pathways of HD over the oxides.

C–Cl and C–S bonds in two molecules of HD, named as addition–elimination (A/E), would form 1,4-dithiane and sesquimustard. Dially sulphide might be originated from sesquimustard through an intra-molecular elimination of HCl. It is important to point out that the distribution or even the kind of HD degradation products could vary along with time-on-reaction due to a further transformation of products into more stable compounds over the oxides. On the other hand, hydrolysis of HD can proceed so long as H_2O presents and it probably benefits by surface base sites, and intra-molecular elimination of HCl is also a major pathway under the action of base sites, while inter-molecular addition–elimination proceeds under the action of surface acid sites. The reaction pathway and distribution of HD degradation products were strongly determined by strength and density of acid–base sites and water adsorbed on the oxides.

5. Conclusion

There wholly exist base sites with more or less number and stronger or weaker strength on the surface of the studied oxides. While no acid sites able to chemisorb NH_3 exist in CaO and MgO. The variation of acid and base sites both in number and strength should relate to the distinctness in the aspects of element, solid structure, impurity, particle (nano-) size and others for the oxides studied. Both acid and base sites over the oxides were not entirely poisoned by H_2O and CO_2 in air and part of them might be unoccupied.

All the oxides studied exhibited room-temperature reactivity for HD adsorbed from droplets as well as adsorbed from vapor. The activity of the oxides towards HD was found to be depended on not only the surface acid–base property but also the adsorbed H_2O. An augmentation of surface acidity or basicity was able to accelerate degradation of HD over the oxides. This degradation appeared to be kinetically profited from an increase of water content in the oxides or reaction temperature. Nanosize alumina was found to have the best activity towards HD with activation energy about 34.2 kJ/mol. Nearly more than 10 kinds of products from hydrolysis, elimination and addition–elimination reactions were detected for HD over the studied oxides. One could speculate that elimination of HCl from HD was accomplished by base sites of the oxides and also possibly by Lewis acid sites of the oxides, intermolecular addition–elimination for HD over the oxides went on through cleavage of both C–Cl and C–S bonds probably under the action of H^+ from hydrolysis and acid sites of the oxides. The hydrolysis rate of HD over the oxides will remarkably increased by water adsorbed on the surface, especially for the base oxides.

Acknowledgements

This work is financially supported by the National Key Fundamental Research program of China (Grant no. 2006CB300401). Prof. Liming Zhou, Prof. Chengxin Pei and Dr. Hongmei Wang are thanked for supplying reference materials and valuable discussion.

References

[1] Y.C. Yang, J.A. Baker, J.R. Ward, Chem. Rev. 92 (1992) 1729.
[2] A. Bellamy, J. Chem. Soc., Perkin Trans. 2 (1994) 2325.
[3] A. Bellamy, React. Polym. 23 (1994) 101.
[4] A. Bellamy, React. Funct. Polym. 32 (1997) 293.
[5] P.W. Bartarm, G.W. Wagner, U.S. Patent 5,689,038 (1997).
[6] D.B. Mawhinney, J.A. Rossin, K. Gerhart, J.T. Yaes, Langmuir 15 (1999) 4789.
[7] K.J. Klabunde, WO98/07493 (1998).
[8] G.W. Wagner, P.W. Bartram, O. Koper, K.J. Klabunde, J. Phys. Chem. B 103 (1999) 3225.
[9] G.W. Wagner, O.B. Koper, E. Lucas, S. Decker, K.J. Klabunde, J. Phys. Chem. B 104 (2000) 5118.
[10] G.W. Wagner, L.R. Procell, R.J. O'Connor, J. Am. Chem. Soc. 123 (2001) 1636.
[11] S. Rajagopalan, O. Koper, S. Decker, K.J. Klabunde, J. Chem. Eur. 8 (2002) 2602.
[12] G.W. Wagner, P.W. Bartram, Langmuir 15 (1999) 8113.
[13] Z.X. Cheng, M. Xu, Q. Chang, H.Y. Zhu, in: Div of NBC Dedfence (Ed.), Supplement to the Proceedings from the 6th CBW Protection Symposium, Stockholm, Sweden, May, 1998, p. 157.
[14] Z.X. Cheng, X.Z. Zhu, G.M. Zuo, G.W. LI, L.Y. Wang, in: FOI NBC Defence (Ed.) Proceedings from the 8th CBW Protection Symposium. Sixth International Symposium on Protection against Chemical and Biological Warfare agents, Gothenburg, Sweden, June, 2004, p. 108.
[15] E.J. Buff, Autosorb1 QA Manual (05300-109), Reversion B, Quantachrome, Chemisorption Part, 2001.
[16] K. Tanabe, T. Yamaguchi, J. Res. Inst. Catal., Hokkaido Univ. 11 (1964) 179.
[17] K. Tanabe, Solid acids and base, first ed., Academic Press, New York, 1970, p. 2.
[18] K. Tanabe, M. Misono, Y. Ono, H. Hottori, New Solid Acids and Bases, Kodansha-Elsevier, 1989,, p. 21.
[19] J. Take, N. Kikuchi, Y. Yoneda, J. Catal. 21 (1971) 164.
[20] S. Tsuchiya, S. Takase, H. Imamura, Chem. Lett. (1984) 661.
[21] C. Walling, J. Am. Chem. Soc. 72 (1950) 1164.
[22] L.P. Hammett, Chem. Rev. 16 (1935) 67.
[23] W. Stumm, J. Morgan, Aquatic Chemistry An Introduction Emphasizing Chemical Equilibria in Natural Water, second ed., John Wiley & Sons Inc., 1981,, p. 462.
[24] J.G. Post, J.H.C. van Hoff, Zerolites 4 (1984) 9.
[25] B. Hunger, J. Hoffmann, Thermochim. Acta 106 (1986) 133.
[26] G. Bagnaco, J. Catal. 159 (1996) 249.
[27] E. Reid, Organic Chemistry of Bivalent Sulfur, vol. II, 1960 (Chapter 5).
[28] D.G. Han, P.L. Gao, Fundamentals of Chemical Kinetics, Peking University Press Company, 1998,, p. 339.
[29] K.J. Klabunde, U.S. Patent 5,990,373 (1999).
[30] I.N. Martyanov, K.J. Klabunde, Environ. Sci. Technol. 37 (2003) 3448.